Management Science Letters 14 (2024) 247–264

Contents lists available at GrowingScience

Management Science Letters

homepage: www.GrowingScience.com/msl

Hybrid optimization model with Neural Network approach for renewable energy prediction and scheduling in large scale systems

Gonzalo E. Alvarez[a*]

[a] *INGAR/CONICET-UTN, Instituto de Desarrollo y Diseño, Santa Fe, Argentina*

C H R O N I C L E

Article history:
Received: December 21, 2023
Received in revised format: January 25 2024
Accepted: February 25, 2024
Available online: February 25 2024

Keywords:
Renewable energy integration
Large-scale power systems
Intermittency
Hybrid modeling
Neural networks
Argentina Electric System

A B S T R A C T

Climate change demands clean energy solutions, and renewable sources such as solar and wind are prime candidates. However, their variability poses challenges for their integration into large-scale power systems. This paper addresses this issue by proposing a novel hybrid mathematical model. The proposal integrates both fossil and renewable sources, considering real-world constraints such as system demand, reserves, and transmission dynamics. The model combines several approaches. By using a novel block composition technique, the computational complexity is reduced, making the model applicable to large-scale systems. A neural network is also developed to improve the forecasting of renewable energy production, which is crucial for managing its intermittency. The effectiveness of the proposed model is tested by considering the large Argentinean electricity system, demonstrating its practical applicability. The results show that acceptable forecasts can be obtained for the generation and transmission scheduling of the whole system.

1. Introduction

When the consequences of climate change are being registered and explained, the need to implement improvements in systems becomes very necessary (IPCC - Contribution of Working Group I to the Sixth Assessment Report of the Intergovernmental Panel on Climate Change, 2021). In this context, technologies that help to reduce carbon dioxide and other greenhouse gases become more interesting (Chen et al., 2016). Consequently, it is essential to have new tools to meet these challenges (BBC, 2021). One of the most important measures taken worldwide is the increase in renewable energy sources at the expense of traditional fossil energy sources, which is closely linked to the increase in environmental reports and measures to reduce the effects of climate change. Renewable energy sources such as solar, wind, hydro, and geothermal provide a sustainable and clean alternative to fossil fuels, significantly reducing greenhouse gas emissions and other atmospheric pollutants (Akella et al., 2009).

The importance of these renewable energy sources has grown significantly in the environment (M. Kumar, 2020). As well as helping to reduce carbon emissions, renewable energy promotes energy independence and security by reducing dependence on imported fossil fuels and the risks associated with changes in oil and gas prices. As well as making a difference in terms of climate change, renewable energy offers significant economic opportunities, creating jobs in local areas and stimulating technological innovation. Several reports predict that thousands of jobs will be created in this area in the future. Advances in the efficiency and cost-effectiveness of renewable technologies are driving rapid growth in the sector. However, the fact that these energy sources are intermittent is one of their main drawbacks (Ahmed et al., 2020). Renewable energy production is

* Corresponding author.

E-mail address: galvarez@santafe-conicet.gov.ar (G. E. Alvarez)

doi: 10.5267/j.msl.2024.2.003

subject to weather and environmental conditions, unlike traditional energy sources such as coal or natural gas, whose availability can be controlled and scheduled.

There are several difficulties with the spread of renewable energy. Firstly, it can lead to fluctuations in energy production, which can affect the stability of the electricity grid and its ability to cover the power demand (Homan et al., 2021). This can lead to unmet demand peaks or excess energy produced at times of low demand, requiring storage or balancing measures to balance supply. Another issue with intermittency is the need for backup systems to ensure a constant supply of electricity. These backup systems typically use conventional power sources, which can increase operating costs and offset the environmental benefits of renewable energy.

However, there are several approaches and solutions to reduce the impact of intermittency on renewable energy sources. One of these is the development of energy storage systems, such as batteries and hydroelectric power (Rakhmonov & Reymov, 2020). These systems allow energy to be stored during periods of high production and released when demand is high. Another approach in which the various renewable sources can be integrated with existing fossil sources is through optimization techniques (Bagherian & Mehranzamir, 2020). There are a large number of papers on optimization, ranging from systems with only thermal sources, such as (R. Kumar et al., 2012), to smart grids where renewable sources are taken into account (G. Alvarez, 2022a). There are also several works analyzing and optimizing not only electricity generation, but also the whole process up to distribution (Arias et al., 2018; Jangir et al., 2023). A complete review of different optimization works related to power systems with different sources can be found in (Abdou & Tkiouat, 2018).

In addition, the implementation of smart grids and demand-side management technologies can improve the flexibility of the power system and optimize the use of renewable energy. With smart devices and automated control systems, these technologies allow energy demand to be adapted to the availability of renewable energy (Poorvaezi Roukerd et al., 2020). In addition, the creation of weather forecasts and predictive models of renewable energy generation can help anticipate fluctuations in production and take preventive measures to ensure a stable and reliable supply (Orlov et al., 2020). Reliable forecasting is essential for identifying improvements in these power systems, both at the design stage and during refurbishment. Renewable generation, particularly wind, is complex, constantly changing, and non-linear (Sinsel et al., 2020). It involves several factors such as climate, altitude, location, and others. There are several methods for predicting renewable energy based on physics, combinations of different approaches, and techniques driven by data analysis. In recent years, data-driven methods have gained popularity due to their efficiency, accessibility, ease of implementation, and potential for more accurate predictions.

There are now a lot of prospects for renewable energy forecasting, thanks to the recent surge in research into neural networks. This approach is useful for dealing with the complexity and unpredictability of renewable energy sources such as solar and wind (Ahmad et al., 2020). They can process large amounts of data on geographical features, historical generation, and weather patterns, revealing subtle relationships that conventional models might miss. In this context, a tool that can learn and adapt to changes is gaining attention: neural networks (Weyn et al., 2020). These can be based on meteorological information, geographical coordinates, and historical energy production, continuously improving their predictions as new data is acquired. By looking at historical records, patterns can be identified that are useful for making predictions (M. Zhang et al., 2021). The ability of these networks to handle large amounts of data makes them interesting for the complex and dynamic field of renewable energy. For example, mathematical models using Artificial Neural Networks (ANN) and Response Surface Methodology have been developed to study the Laser Direct Structuring process, a process used in the manufacture of electronic devices and high-tech electronic products (Bachy & Franke, 2015). In (Sahoo et al., 2015), a model using neural networks is developed to predict surface roughness with higher accuracy in the field of 3D printing, highlighting the superiority of the neural network model over the traditional methodology.

In this regard, the novel proposal introduces a mathematical model that allows the scheduling of a large electrical system, emphasizing the randomness of renewable energy. For the power system, real constraints such as system demand, reserves, balances, power transmission, and the characteristics of each generation source are considered. In view of the above, this article reduces the gap by presenting the following contributions:

-Develop a novel hybrid mathematical model capable of organizing the electrical production of a large electrical system, considering not only fossil sources, which can be considered as having a certain flexibility of generation, but also renewable sources, which are characterized by their intermittency. It considers thermal generation by plants using natural gas and other fossil fuels. These sources are joined by wind and solar, which are the most important in the world. The work also includes the dynamics of electricity transmission.

- For attending to the complexity of a large-scale system, is a model that considers the power generation in the form of block composition. This method reduces the computational effort required to solve the scheduling problem.

- For the planning of renewable generation, the development of a neural network to predict wind energy production is presented. This advance is fundamental in a context where the management of renewable energies such as solar and wind requires

precise tools to deal with their intermittency and variability, thus contributing to better planning and management of energy resources.

- To reduce the computational effort, techniques are used that allow simplifications, but with a sufficient level of accuracy and realism.

The developed model is applied to a large practical case, specifically the Argentinean Electric System. This system was chosen because of its integral representation of the different types of energy generation that make up almost the entire national energy matrix. It also stands out for its extensive transmission infrastructure, with more than 14,197 km of high-voltage lines and an installed thermal generation capacity of more than 40 GW. This system supplies energy to a population of 45.8 million and its industries, as well as to neighboring countries.

The remaining sections are organized as follows. Section 2 presents and describes the novel mathematical model. Section 3 presents the deep learning mixed model. The modified test system is presented and described in Section 4. The results are evaluated in Section 5. Finally, some conclusions are presented in Section 6.

2. Operation block model for large-scale systems

With generators arranged by region, **Fig. 1** aims to provide a better understanding of the modeling of a large-scale system. There are 3 generating blocks and three buses in the system. Blocks and loads are connected to each of the buses 1 and 2. In Block 1, there are two hydroelectric units, three nuclear plants, four photovoltaic plants, four wind turbines, and three natural gas thermal plants. Block 2, which has two nuclear power plants, two gas natural units, one wind turbine, two hydro plants, two PV plants, and two non-gas thermal units, is connected by Bus 2. Bus 3, on the other hand, has a load with 2 natural gas units, two non-natural gas units, one wind turbine, and one PV plant. This method has been useful tested for solving large systems in previous works as (Alvarez, 2020a; Alvarez, 2021).

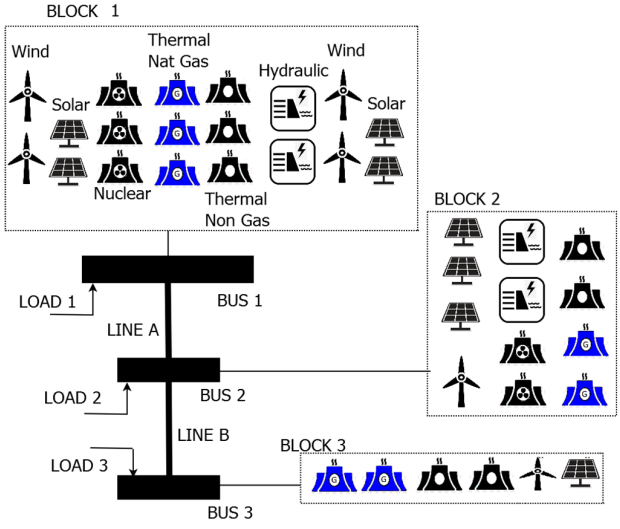

Fig. 1. Scheme of a system with the framework by using a method based on block arrangement.

2.1 Power generation model

The goal function is to reduce the overall cost of electricity production through operation. The period, one hour, is specified for the programming horizon, T, which is set to 24 hours. The total of the variables about the power output for each source—thermal units powered by natural gas, thermal units powered by other fossil fuels like diesel, hydropower plants, photovoltaic units, nuclear power plants, and wind turbines—makes up the objective function. Each generation technology-associated generation costs are compounded by all power outputs. where *I* is the total number of blocks of generators and i is the set that corresponds to each block of generators. Where $\rho^g/\rho^{ng}/\rho^h/\rho^n/\rho^w/\rho^{pv}$ are constants of fuel cost function coefficients gas, non-gas, hydro, nuclear, wind, and PV types ($/MWh), and p is the power production (MW).

$$min\ F\ = \sum_{t=1}^{T}\sum_{i=1}^{I} p_{i,t}^{g}\rho^{g} + p_{i,t}^{ng}\rho^{ng} + p_{i,t}^{h}\rho^{h} + p_{i,t}^{n}\rho^{n} + p_{i,t}^{w}\rho^{w} + p_{i,t}^{pv}\rho^{pv} \quad (1)$$

The sum of the power outputs from all the blocks that correspond to bus *bu* equals the overall power output that the bus generates ($p\_total_{bu,t}$).

$$p\_total_{bu,t} = \sum_{i \in bu} p_{i,t}^{g} + p_{i,t}^{ng} + p_{i,t}^{h} + p_{i,t}^{n} + p_{i,t}^{w} + p_{i,t}^{pv} \ , \quad t = 1, \dots, T \tag{2}$$

According to system demand constraint (3), the total power output across all buses must be sufficient to meet the overall electricity consumption. The total of all the loads makes up the total demand. BU is the total amount of buses, C is the total amount of loads, and bk is the power consumption (MW).

$$\sum_{bu=1}^{BU} \sum_{c=1}^{C} bk_{c,bu,t} \leq \sum_{bu=1}^{BU} p\_total_{bu,t} \ , \qquad t = 1, \dots, T \tag{3}$$

The power that is available but hasn't been charged for the system is known as the spinning reserve (4), and it can react quickly to make up for any transmission or generation faults in the future. Two presumptions will be made in this essay. Initially, 10% of demand will be anticipated for the spinning reserve. Furthermore, due to the large number of generators in each block, there is sufficient spinning reserve in every block. Where

$\overline{p\_total_{bu}}/\underline{p\_total_{bu}}$ are the upper and lower bounds on total power (MW).

$$R_t \ \leq \sum_{bu=1}^{BU} \overline{p\_total_{bu}} - \sum_{bu=1}^{BU} p\_total_{bu,t} , \qquad t = 1, \dots, T \tag{4}$$

There are lower and maximum bounds on the power output. Furthermore, every technology that makes up the block generators.

$$\overline{p\_total_{bu}} \leq p\_total_{bu.t} \leq \underline{p\_total_{bu}}. \qquad t = 1. \dots . T; \ bu = 1, .., BU \tag{5}$$

Each thermal unit of the dispatch problem must take into account a number of variables, including starting, shutdown, down/up ramps, hot/cold start costs, and minimum/maximum on/off status times. The restrictions that take these things into account are described in (G. Alvarez, 2020a). They are not covered in this study since it considers generation by block, and each block has a large number of units.

2.2 Nuclear generation

There are currently 453 nuclear reactors in the globe, spread over 31 nations, with a total installed capacity of 397,477 MW. One unique feature of nuclear generating is that its minimum operation and shutdown times typically range from 24 to 48 hours (Panos & Lehtilä, 2016). Because of this, it is difficult and expensive to change the generation of these plants; so, their operation is maintained steady for an extended period with minimal generation level volatility. Depending on its design, nuclear reactors can be of numerous sorts and are used to generate electricity (Breeze, 2014). Heat is transferred from the Pressurized Water Reactor to a high-pressure water reservoir, which then transfers the heat to a secondary circuit. The steam created by this final circuit goes into a turbine to generate energy. The majority of the world's reactors are found in Germany, the United States, and France.

The second most popular kind worldwide is the Boiling Water Reactor, which generates steam for a turbine. The fact that refueling the reactor requires stopping it is a drawback. Some of the other reactors are the Uranium Gas and Graphite Reactor, which uses gas as coolant and graphite as moderator; the Advanced Gas Reactor, which is widely used in Britain; the Heavy Water Nuclear Reactor, which uses heavy water as moderator and coolant; and the Fast Breeder Reactor, which does not use neutron moderator. However, nuclear power plants make up a sizable share of the energy mix in some nations. In these situations, developing a load of some kind after nuclear units are required. Pressurized Water Reactor reactors have regulation range capacities of up to 5% of the nominal power every minute since they are the most common reactors in the world and have more than 40 years of experience in the load following (Zhao et al., 2014). Nuclear power plants can therefore be run in three different modes: load following, primary and secondary frequency control, and base-load generation (Nuclear Energy Agency, 2011). When functioning in this mode, the units are using their rated power. Although, in theory, it is the most efficient mode of operation, it cannot handle consumption surges. It is determined that, if this kind of operating mode is selected, where a nuclear unit's rated power is represented by Pn_i^r. Constraints for the rest of the operating mode of nuclear units can be found in (Alvarez, 2022b).

$$p_{i,t}^{n} = Pn_i^r \qquad , i = 1, \dots, I; t = 1, \dots, T \tag{6}$$

2.3. Hydro Power Generation and Pumped Storage

The results of relationships between variables for power produced-water discharge are used to create the operating curves of hydroelectric power plants, which are dependent on reservoir restrictions (Li et al., 2014). They have nonlinear features and, for technical reasons, are not allowed to be used as work zones. In addition, the dispatch problem as it relates to hydro generation considers the relationship between the early and last hours of the programming horizon. This relationship conditions all hydro generators and reservoirs and is provided in the form of initial values. Furthermore, there exist connections between the ensuing epochs. As a result, there are multiple periods involved in the problem, and the generation at different times depends on the values that came before and after (Alguacil et al., 2000).

According to (C. H. Chen et al., 2017), the limitation that initially represents the power production from hydraulic sources is non-linear. Bilinear terms related to turbine flow and hydraulic head are present in this limitation. The Mixed Integer Linear Programming model will be obtained by approximating it linearly using regions that follow the model of (G. Alvarez, 2020b). The consideration of the consequences of variations in hydraulic head, which are sometimes overlooked in the literature, is ensured by this model. Compared to other methods, this one also needs fewer auxiliary variables to linearize the operation curves.

In fact, pumped storage systems use energy instead of producing it when they are pumping. In any event, they need to be examined because failing to do so will make it impossible to use the results in actual systems. The original constraint, which indicates the power used to pump water when the machine is in pumping mode, is non-linear. It deals with the product of the hydraulic head variable and the pumped flow variable, two continuous variables. It is expected that there be many leap levels for the pumping mode, much as there are for hydro generation. However, compared to the generating mode, the working range for the pumping mode is often shorter. For a linearization of this constraint, see (Alvarez, 2020b).

In the mentioned work several constraints are developed as a new contribution, ensuring that the weight variable representing the operating point in pumping is located correctly. It considers the hydraulic head effects brought about by the variation in reservoir heights. A Binary variable is considered, which has an operating range defined by the new constraints, which is 1 when the head level corresponds to a specific segment in time. The variations in reservoir volumes show the levels of heads. The mentioned method is illustrated in **Fig. 2**.

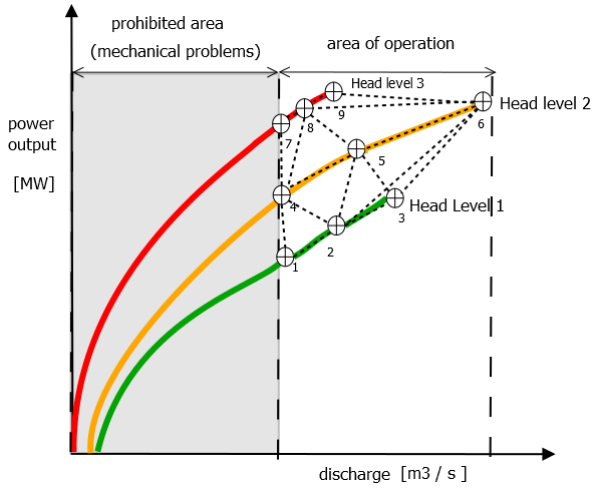

Fig. 2. Linearization method of hydropower generation.

2.4. Photovoltaic (PV) Generation

The formulation of the operation of PV units must consider perturbations caused by various environmental conditions, including clouds, the temperature impacts of each region, and obstructions. This challenge is addressed by both stochastic and deterministic models. To maximize the effectiveness of the solar radiation they gather; photovoltaic facilities are typically situated in areas with a high number of sunny days. There are two parts to the solar radiation that the planet receives. The direct component is the irradiance projected in a straight line from the sun to the collector surface Because of physical phenomena like scattering, the other component, the diffuse irradiance, lacks a defined direction. It is shown that the power generation level is nearly related to the time factor when the daily scheduling of this generation source for large-scale systems is examined. This is a result of the thoughtful placement of these plants. According to statistics provided by the Independent Operator (ISO) of the Argentinean Electric System, **Fig. 3** depicts the power generated per hour for the PV generation in the electric system of Argentina graphically for 1 August 2023.

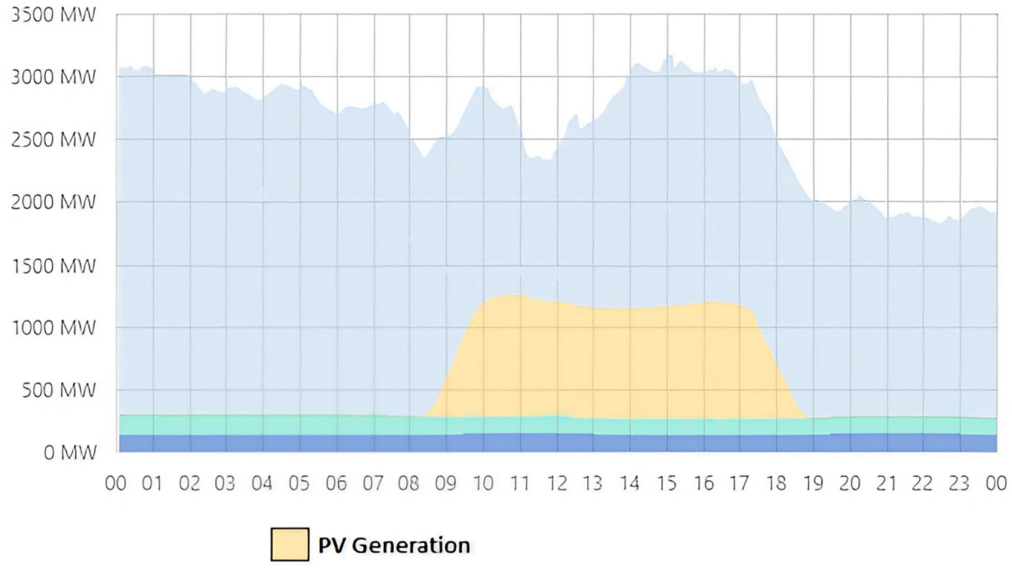

Fig. 3. Daily PV generation in Argentina, based on its ISO (CAMMESA, 2023)

As evident from the analysis of several days of PV source programming, a significant resemblance exists among different days within the same season for this energy source. Production initiates at sunrise, peaks around noon, sustains for several hours, and gradually declines, concluding at sunset (Branco et al., 2020). This pattern is attributed to the fact that, in large-scale systems, the majority of PV farms are strategically located in areas characterized by numerous days of solar availability. Consequently, in alignment with the established framework presented in (G. Alvarez & Blas, 2021), it is proposed that solar production follows a consistent curve with minor variations for a given season. Additionally, it is imperative to underscore the reliability and constancy of this solar production trend, underscoring the negligible deviations encountered. This consistency lends itself to enhanced predictability and efficiency in managing solar energy resources. Furthermore, understanding and leveraging these patterns are crucial for optimizing the design and operation of solar energy systems, and fostering advancements in engineering practices within the renewable energy sector (Wang et al., 2020).

2.5 Wind Generation

There can be wide variations in wind speed. Consequently, patterns of behavior can be determined based on a variety of parameters, including land relief, altitude, and geographic zone. The following represents how much wind power a turbine can generate (p^w is the power output in W):

$$p_i^w = \frac{\mathrm{A}\ \delta\ \mu^3}{2} \tag{7}$$

where μ is the wind speed in meters per second, δ is the air density, expressed in kg/m^3, A is the area that crosses the wind in m^2. The working principle of a wind turbine, comprising an electric generator, a reduction box, and a rotor that harvests wind energy, is explained in (Burton et al., 2011). A horizontal axis is present in the vast majority of turbines. Through the gearbox, the mechanical torque generated by the wind in the rotor is transferred to the electric generator. Turbines can be divided into two categories based on the angle at which they operate: fixed turbines, which depend on the frequency of the main system, the gearbox, and the specifications regarding to generator in order to maintain the rotor speed regardless of wind speed. Additionally, there are variable-speed wind turbines that reduce wind speed changes by altering the rotational speed of the wind turbine. These wind turbines rely on a control system to maintain the mechanical torque of the rotor. Since they utilize the wind more effectively, the latter type of turbine is the most common.

Many works suggest that it is reasonable to assume that constraint (8), with a moderate (and large) contribution from PV generation to the total matrix, may be achieved with an appropriate level of precision for large-scale system daily scheduling. According to this constraint, the incidence matrix, $\Gamma_{i,t}^w$, with coefficients corresponding to each block ranging from 0 to 1, would define the maximum power output, $p_i^{w\_max}$. When developing the matrix, season-specific changes, climatological forecasts, and the average number of days elapsed are all taken into account.

$$p_{i,t}^w \leq \Gamma_{i,t}^w\ p_i^{w\_max} \qquad ,i = 1, \dots, I; t = 1, \dots, T \tag{8}$$

Online generation projections will be deployed to wind farms by systems operators using prediction tools. These predictions are updated hourly or even, each minute, and the most recent data is appended to the prediction models (Foley et al., 2012;

Neshat et al., 2021). Operators of wind farms typically have access to the forecasts needed to operate their contribution to the grid. This last topic will be discussed in more detail in the following section.

2.6 System operation

The DC flow model (Stott et al., 2009) is chosen to handle power transmission representations. Its primary advantage is that it requires less computational effort and can produce workable solutions that are nearly identical to those of the non-linear AC model (Overbye et al., 2004). In (Van Den Bergh et al., 2014), the model is explained in detail. (9) models the power flow carried by the line connecting bus bu_i and bus bu_o. Where $p\_l_{bu_i,bu_o,t}$ is the power transferred between buses (MW), $\theta_{bu_i,t}/\theta_{bu_o,t}$ is the Angle of the input/output bus voltage (rad), and R_{bu_i,bu_o} the reactance.

$$p\_l_{bu_i,bu_o,t} = \frac{\theta_{bu_i,t} - \theta_{bu_o,t}}{R_{bu_i,bu_o}}, \quad t = 1, \dots, T \tag{9}$$

Eq. (10) shows the balance for each bus in terms of power. It stipulates that the total power generated and transmitted must match the total power stored and used, where $c_{bu,t}$ is the bus power consumption (MW), and $SP_{bu,t}$ is the Power storage in a bus (MW).

$$p_{bu,t}^{total} + p\_l_{bu_i=bu,bu_o,t} - p\_l_{bu_i,bu_o=bu,t} = c_{bu,t} + SP_{bu,t}, \quad t = 1, \dots, T \tag{10}$$

3. Deep Learning for Renewable Energy forecast

The prediction of renewable wind energy using deep learning will be the main topic of this section. Numerous studies have shown that wind energy is unique among sources that are highly random. Therefore, deep learning techniques will be applied to a time series database to improve forecast accuracy. Because wind energy is inherently unpredictable, accurate forecasting is difficult. Deep learning methods, known for their ability to identify complex patterns in data, offer a viable way to increase the accuracy of wind energy generation forecasts.

The process used is shown in **Fig. 4** and consists of several steps. The first step is to acquire a database, the size and content of which is determined by the intended forecast horizon. Databases can vary, but certain basic data parameters must be included. These include wind direction and speed, the date and time of production, and the amount of power produced - both theoretical and actual. The database must then be analyzed to find any missing or erroneous data. Inaccurate data, such as wind speeds above 3m/s with no power output, may indicate that the turbine needs maintenance, and missing data can be approximated. This is an important aspect to recognize and deal with, as it can adversely affect neural network training. Furthermore, the calculation of features useful for analysis, including power loss (real and theoretical), is another essential step (Kim & Kim, 2020).

A statistical function called autocorrelation measures the linear relationship between the values of datasets and their own lag (previous) values. To put it another way, autocorrelation shows how similar a variable's values are throughout time. Autocorrelation is a commonly used tool in temporal statistics and time series analysis for examining patterns and trends in sequential data. It is feasible to determine whether or not there is a significant connection between the time series values at different time intervals by computing autocorrelation (Yeh et al., 2023). By revealing the temporal dependencies present in data, this analytical method helps to shed light on the dynamics and behavior of the underlying processes throughout time. Its implementation is essential because it allows for a more comprehensive comprehension of the temporal structure of data, improves modeling and prediction capabilities, and helps to validate statistical hypotheses. Utilized across a wide range of disciplines, from meteorology to econometrics, its application greatly aids in making well-informed decisions. In order to effectively understand and describe sequential data, analysts and decision-makers can benefit from autocorrelation's ability to reveal temporal patterns and connections. The knowledge obtained by autocorrelation analysis is essential for forecasting, model improvement, and guaranteeing the validity of statistical conclusions, all of which contribute to rational decision-making in a variety of fields.

When two or more time series show stochastic patterns and are not separately stationary, they are said to be cointegrated. This is a long-run statistical relationship. A set of two or more non-stationary time series is said to be cointegrated if a linear combination of them produces a stationary series. Cointegration suggests that the time series have a long-run relationship over time. A more detailed explanation of cointegration can be found in (Carrion-i-Silvestre & Kim, 2019).

When dealing with time series data, a stationarity test is essential to ensure that the data retain their statistical properties over time. Forecasting models may not be as reliable if a time series is not stationary. The term 'stationarity' refers to the fact that the statistical properties of the series, such as its mean and variance, are constant over time (Livieris et al., 2020). The Augmented Dickey-Fuller (ADF) test is a commonly used tool in this area to assess the stationarity of a time series (Silva et al., 2021). The purpose of the ADF test is to identify unit roots in a time series, which indicate a trend and hence non-stationarity.

If there is a long-term trend in wind power generation, stationarity becomes even more important. The ADF test can help determine if there is a significant trend and, if so, how to resolve it to improve the model's predictive ability. Understanding and ensuring stationarity in time series data is critical to creating reliable predictive models in the renewable energy sector, such as wind power generation. Engineers and analysts can use the ADF test to determine if patterns exist and make informed adjustments to increase the accuracy of predictive models. By carefully accounting for stationarity, models are more reliable and efficient in predicting wind power generation patterns over time.

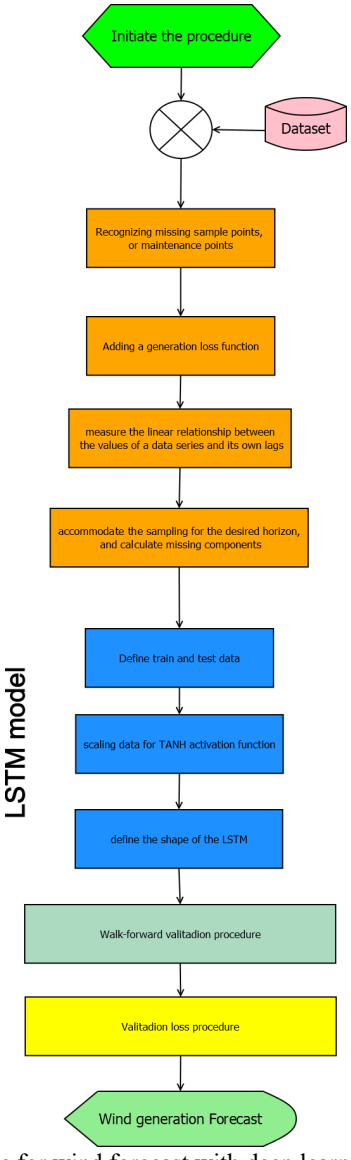

Fig. 4. Scheme for wind forecast with deep learning procedure.

The development of an artificial recurrent neural network model for Long Short-Term Memory (LSTM) prediction then begins. A great deal of thought is required when partitioning the data. Separating the data into training and test sets is the first step (Kagemoto, 2020). Typically, about 80% of the data is set aside for training and the rest for testing. Since LSTM uses a hyperbolic tangent (tanh) activation function, the data is then normalized to a range between -1 and 1 (Sun et al., 2018). Finally, three layers - samples, time steps, and features - should form the LSTM network structure (Yan & Ouyang, 2018). By following industry best practices for neural network construction and data pre-processing, this comprehensive method ensures that the model is ready for training and prediction. Using LSTM networks, the walk-forward validation method appears to be a successful approach for predicting wind power generation. This method allows the model to be continuously adjusted in response to new data, improving forecast accuracy and the model's resilience to changing circumstances. This strategy is very useful when using LSTM networks. It involves using past data up to a given point in time to train the model, and then evaluating how well it predicts data for the next period. In the field of wind power forecasting, walk-forward validation helps to produce more reliable and adaptive predictions by allowing the model to adapt dynamically to changing data patterns (Zhang et al., 2019). The time window is then advanced, new data is added, and the model is then retrained. This

process is repeated until the end of the dataset. This approach is advantageous for a number of reasons, one of which is that it allows the model to continuously adapt to variations in the pattern of wind power output over time. This flexibility is essential as changing weather patterns can have an impact on wind energy production. Accurate prediction and a continuous and progressive evaluation of the model's ability to generalize are made possible by testing it with updated data at each stage. As new data is added, the model continuously improves its performance by dynamically adapting. The use of an iterative process ensures that the prediction model remains accurately calibrated to the changing characteristics of wind power generation over time (Farrokhtala et al., 2019). A full paper discussing in detail each stage of the wind power prediction process using LSTM networks can be found in (Bharadwa, 2020).

4. Test case

The Electric System of Argentina is mainly thermal (using natural gas), with a large amount of hydroelectric power, which is above the world average. The system is divided into nine regions: Patagonia (PAT), Greater Buenos Aires (GBA), Buenos Aires (BGA), Comahue (COM), Northwest Argentina (NOA), Northeast Argentina (NEA), Cuyo (CUY), Centre (CEN), Litoral (LIT) and Greater Buenos Aires (GBA). Each region has unique characteristics in terms of installed capacity, consumption trends, and generation types. The appendix in (G. Alvarez, 2020a) provides a detailed breakdown of the electricity distribution by region, based on installed capacity (CAMMESA, 2019). The same report also documents the corresponding electricity consumption data. It is noteworthy that the Greater Buenos Aires (GBA) region, where ISO CAMMESA controls each region like a monopoly, has a concentration of more than half of the demand.

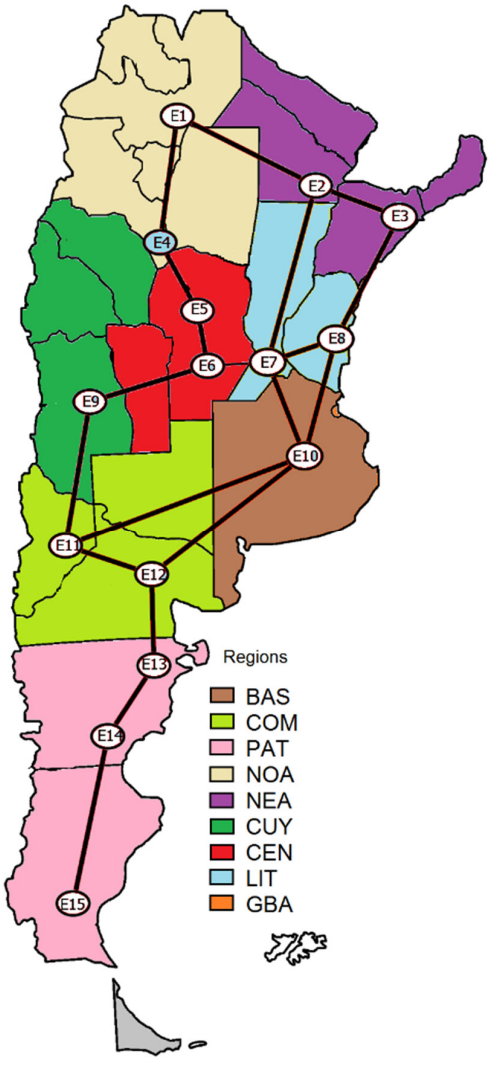

Fig 5. Scheme of the 500 kV Argentinean Electric Power System

According to (Argentine Atomic Energy Commission (CNEA), 2016), the energy sources of the country are as follows: nuclear 4.7%, hydro 29.1%, other renewables 2.4% and fossil fuels 63.8%. Wind 53%, hydro < 50 MW 32.9%, biogas 3%, biomass 3.1%, and photovoltaic 8% are the subcategories of other renewables. Natural gas accounts for 90.1% of fossil fuels,

diesel for 4.5%, coal for 2.1%, and fuel oil for 3.3%. As far as energy transmission is concerned, a transport network of more than 12,000 km of lines at 500 and 220 kV is supervised by TRANSENER, which operates under a TRANSCO figure (Shahidehpour et al., 2003). Information on the main transmission lines can be found in (G. Alvarez, 2020a). Because of this complex energy landscape, it is important to have a thorough understanding of the regional dynamics, which highlights the vital role that electrical infrastructure plays in maintaining the power grid. In terms of nuclear power generation, Argentina has three nuclear reactors. The first, Atucha I, located in the province of Buenos Aires, was inaugurated in 1974 and has an installed capacity of 362 MW. Atucha II, located in the same area, is another plant using natural uranium as fuel and has been in operation since 2006. It has an installed capacity of 745 MW. The province of Córdoba is home to Embalse, a third nuclear power plant with an installed capacity of 648 MW. Where more than one substation is associated with a single region, the performance statistics of each substation took into account the zone-specific data provided by CAMMESA and other organizations. The production costs indicated in the objective function (1) are taken from (U.S. Energy Information Administration, 2017), which provides information on the costs associated with different generation sources, including fuel consumption, maintenance, and construction. **Fig. 5** provides more details on the electrical system by showing important substations (E1-E15, which will be designated as buses) with 500 kV lines and highlighting the different geographical areas that make up the system. The electrical system data that was utilized for this study can be found in (G. Alvarez, 2020a) and pertains to April 2019. Furthermore, the generation forecast of the system is created at 12:00 PM the day before dispatch. With 5-minute time update intervals, load dispatch is continuously modified in real-time based on actual availability.

The optimization model that will be in charge of cargo dispatch planning for the entire country will be programmed using PYOMO optimization software (Hart et al., 2011). This is an open-source code program built on the Python programming language that is used to formulate and solve optimization problems. Widely applicable to a variety of problems, it can be used for linear, quadratic, non-linear, integer, and stochastic programming. The detailed way in which this large-scale system has been optimized is described in detail in (G. Alvarez, 2020c, 2020a).

Regarding the prediction of wind generation, the wind turbine database found in (Erisen, 2018), which is free and publicly available, is used for this purpose. This database was recorded every 10 minutes from 1 January 2018 to 31 December 2018, it also has data of active power, wind speed, theoretical power, and wind direction. **Table 1** shows the first records of this database and the total record for the whole year is plotted in **Fig. 6.**

Table 1
First wind turbine database records.

Date/Time	LV ActivePower (kW)	Wind Speed (m/s)	Theoretical_ Power_Curve (KWh)	Wind Direction (°)
01 01 2018 00:00	380.0477905	5.31133604	416.3289078	259.9949036
01 01 2018 00:10	453.7691956	5.672166824	519.9175111	268.6411133
01 01 2018 00:20	306.3765869	5.216036797	390.9000158	272.5647888
01 01 2018 00:30	419.6459045	5.659674168	516.127569	271.2580872
01 01 2018 00:40	380.6506958	5.577940941	491.702972	265.6742859
01 01 2018 00:50	402.3919983	5.604052067	499.436385	264.5786133
01 01 2018 01:00	447.6057129	5.793007851	557.3723633	266.1636047
01 01 2018 01:10	387.2421875	5.306049824	414.8981788	257.9494934
01 01 2018 01:20	463.6512146	5.584629059	493.6776521	253.4806976
01 01 2018 01:30	439.725708	5.523228168	475.7067828	258.7237854
01 01 2018 01:40	498.1817017	5.724115849	535.841397	251.8509979
01 01 2018 01:50	526.8162231	5.934198856	603.0140765	265.5046997

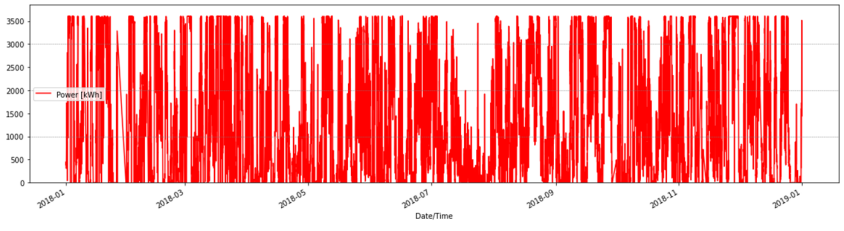

Fig 6. Wind registers from 1 Jan 2018 to 31 Dec 2018.

The following steps for processing the dataset are carried out using Python in Spyder (Raybaut, 2009). As a result, several modifications were made to the acquired data to obtain usable information for the application of the novel method. First, observations with a wind speed greater than 3.3 m/s and a power output of zero were excluded, indicating that the system was likely in maintenance mode. This decision assumed that these events were likely to be associated with scheduled maintenance.

After eliminating these observations, the remaining dataset was retained to allow the model to accurately represent and predict intermittency in wind power production. This tactical technique allows a deeper understanding of the inherent variability in the data.

The data were resampled on an hourly basis to improve the predictability of the model and to provide a more consistent analysis. At the same time, missing values were methodically interpolated to make the data more consistent and comprehensive for subsequent analysis. A key addition to the dataset was the addition of a new feature showing the difference between actual and theoretical performance. This additional feature sometimes referred to as 'loss', provides important information about the discrepancy between measured and expected power generation. To understand how wind direction affects power generation results, a category feature has been carefully designed. This feature helps to provide a more detailed knowledge of the directional dynamics affecting wind turbine performance by classifying wind direction into discrete cardinal points (e.g. North, Northeast, East). This unique category feature is a critical component of the input, adding to its complexity and comprehensiveness as a predictive framework.

An extensive analysis of the Autocorrelation Function (ACF) and the Partial Autocorrelation Function (PACF) is then carried out. This thorough analysis will allow me to identify and understand the temporal correlations and patterns present in our dataset. The ACF and PACF analyses will allow us to find connections between observations at different time lags, which will also provide important insights into the temporal structure of the data. This thorough analysis is an important first step in improving the understanding of time series dynamics. **Fig. 7** shows both ACF and PCAF functions. A clear correlation between the time step at t-1 and the observed time step (t) can be seen in the ACF plot. The visual representation implies a significant dependence on the previous time point, t-1, demonstrating a temporal pattern or correlation in the data. The PACF plot shows the association between an observation and several previous time steps, in this case over a period of 30 days. The graphical representation of PACF highlights that a time lag of 1-time step has the greatest significance. All this suggests that it would be interesting to add a column to the dataset with the production value of the previous hour.

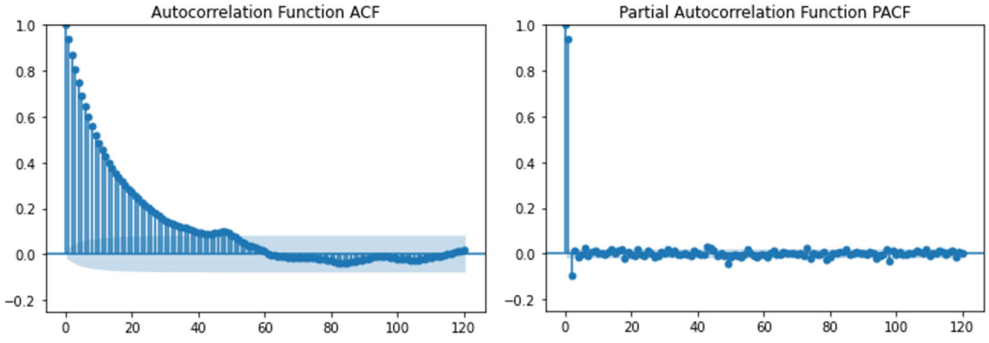

Fig 7. Autocorrelation and Partial Autocorrelation functions over 120 days.

To properly model time series data, it is essential that the data exhibit stationarity. The concept of stationarity suggests that basic statistical properties, such as variance and population mean, are constant over time. This property is important because many statistical models and analytical tools depend on it to make a correct prediction (Horváth et al., 2014). Each time series characteristic in the dataset was tested for stationarity using the Augmented Dickey-Fuller test (Phillips & Ouliaris, 1990). There are two hypotheses Ho: the time series is assumed to be non-stationary and to have a unit root if the hypothesis is not rejected. This indicates the existence of a time-dependent structure. And H1: If the null hypothesis is rejected, it means that there is no unit root in the time series, i.e. it is stationary with no time-dependent structure. If the p-value is less than or equal to 0.05, the null hypothesis is rejected, otherwise, it is not. In the case of this database, all the p-values for wind speed, theoretical power, loss, and wind are less than 0.05. The test therefore proves stationarity.

A detailed summary of the most common wind patterns for the whole year is shown in **Fig. 8**. The eastward path is at the center of the figure, with the arrows clearly indicating the direction of the wind. Understanding these orientations is essential to understanding the cyclical and predictable behavior of the wind over a given period. Revealing the dominant wind patterns provides insightful information that can be used in a variety of contexts, from environmental impact studies to the optimization of wind energy systems.

The essential procedures for building a deep learning model are described below. The first step in these procedures is to carefully partition the data into training and test sets, ensuring that the latter preserves the integrity of the model. Data partitioning is done rigorously to protect the integrity of the training data from possible contamination by the test data. The complete data set is first partitioned into training and test sets. Thanks to the 2018 dataset, all data points from 1 January to 30 November are used for training, and only testing data are used in December (based on the criteria of (Bharadwa, 2020)). Furthermore, this work only predicts a short time horizon. The datasets are then customized to meet the specific needs of the

model. The proposed predictive model architecture uses a Long Short-Term Memory (LSTM) artificial recurrent neural network. The ideal model configuration is found through hyperparameter tuning guided by relevant metrics.

For LSTM models, data scaling is essential to ensure that values are within the -1 to 1 range specified by the default TANH activation function. The characteristics of the modified hourly data set include 'real power (kWh)', 'wind speed (m/s)', 'theoretical power (kWh)', 'power loss (kWh)', 'x component for wind direction', 'y component for wind direction' and 'real power of previous step'.

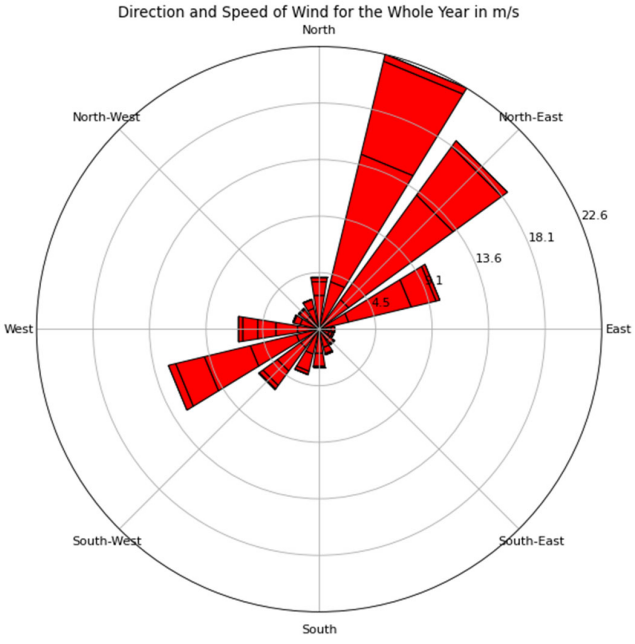

Fig. 8. Windrose map of wind activity (speed and direction).

According to Brownlee (2017), to meet the specifications of long short-term memory (LSTM) models, the data are pre-processed and organized into a three-dimensional format, referred to as "data", "time steps" and "features". The training and test data sets are divided into two groups. At the end of each period, each sequence is used as input to predict the target variable. The use of the walk-forward validation method makes it possible to make hourly predictions that are updated. In this case, the time step of the considered case is 24 (24 hours x 1 day) since the programming horizon is 24 hours. The optimization of several hyperparameters is essential for the performance of the LSTM model. Mean squared error (or simply MSE) was used as an evaluation metric to compare predictions on the validation set to assess the performance of this regression method. The following hyperparameters made up the final model configuration with a particularly low MSE on the validation data (based on suggestions from the work of (Bharadwa, 2020)): Batch size 14, epochs 35, neurons 32, layers 2, dropout rate 0.05, and the ADAM optimizer is selected. The code is shown in detail in **Fig. 9**.

```
import tensorflow as tf
from tensorflow.keras.layers import RecurrentLayer, DenseLayer, RandomDropout
from tensorflow.keras.callbacks import TerminateEarly

def construct_tailored_model(input_sequences, target_values):
    recurrent_cells = 32
    recurrent_dropout = 0.05
    training_iterations = 35
    training_chunk_size = 14
    tailored_optimizer = tf.keras.optimizers.Adam(learning_rate=0.0005)
    early_termination = TerminateEarly(patience=7, monitor='loss')

    model = tf.keras.Sequential()
    model.add(RecurrentLayer(units=recurrent_cells, dropout=recurrent_dropout, return_sequences=True,
                             input_shape=(input_sequences.shape[1], input_sequences.shape[2])))
    model.add(RecurrentLayer(units=recurrent_cells, dropout=recurrent_dropout))
    model.add(DenseLayer(units=1))

    model.compile(optimizer=tailored_optimizer, loss='mean_squared_error')

    return model
```

Fig 9. Code for the creation of LSTM model.

Walk-forward validation is used to continuously check performance. This iterative approach continuously evaluates and refines the model by incorporating new data as it becomes available. The model generates predictions for the most recent observations and is periodically retrained on past data using a rolling window technique. This continuous process, which mimics the real world where predictions are made sequentially, provides important insights into the model's ability to generalize to unknown data. Finally, the data points that have been transformed into -1 and 1 values need to be rescaled between the correct values.

During model training, it is necessary to carefully monitor how well the model has learned from both the training and validation data. This is done by keeping a detailed record of a metric called Mean Squared Error (MSE), which measures how far the predictions are from the actual values. But consistency is not enough, you also want the model to perform well on new data it has never seen before. This is where the validation data set comes in: it provides a reality check on how well the model generalizes. The training and validation procedures converge at a value of 0.063.

5. Results

The predicted wind power for one turbine is shown in **Fig. 10**, the value has been taken as a unit so that it can be extrapolated to all regions of the system. There is an acceptable degree of approximation between the two curves, there is a small "overtaking" of time that occurs from hour 6 where the prediction is ahead of the actual power.

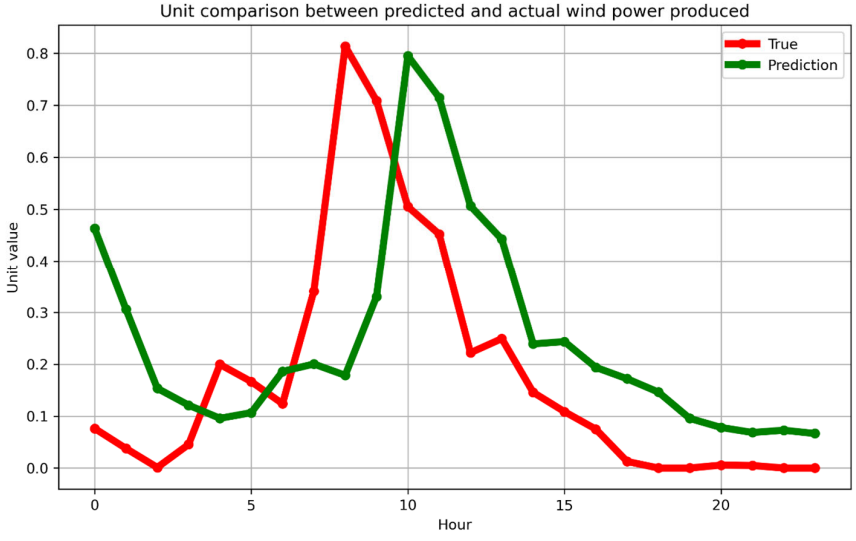

Fig 10. Unit comparison between real and predicted power output for wind generation.

Fig. 11 shows a screenshot of the ADAM optimizer solving the overall system scheduling after considering the wind production predictions made previously for the wind sources. The mathematical model before pre-processing has 5257 equations and 2977 variables. The total generation cost is USD 6,844,695.

```
GLPSOL--GLPK LP/MIP Solver 5.0
Parameter(s) specified in the command line:
 --write C:\Users\gonzalo\AppData\Local\Temp\tmpz21x0ld7.glpk.raw --wglp C:\Users\gonzalo\AppData\Local\Temp\tmpe5pe2cle.glpk.g
lp
 --cpxlp C:\Users\gonzalo\AppData\Local\Temp\tmp50iwva8r.pyomo.lp
Reading problem data from 'C:\Users\gonzalo\AppData\Local\Temp\tmp50iwva8r.pyomo.lp'...
5257 rows, 2977 columns, 8665 non-zeros
29580 lines were read
Writing problem data to 'C:\Users\gonzalo\AppData\Local\Temp\tmpe5pe2cle.glpk.glp'...
24415 lines were written
GLPK Simplex Optimizer 5.0
5257 rows, 2977 columns, 8665 non-zeros
Preprocessing...
744 rows, 1716 columns, 2892 non-zeros
Scaling...
 A: min|aij| =  1.000e+00  max|aij| =  1.000e+00  ratio =  1.000e+00
Problem data seem to be well scaled
Constructing initial basis...
Size of triangular part is 744
      0: obj =   1.228339000e+07 inf =   6.132e+05 (288)
    189: obj =   1.228339000e+07 inf =   2.740e-11 (0) 1
*   974: obj =   6.844695794e+06 inf =   1.403e-11 (0) 2
OPTIMAL LP SOLUTION FOUND
Time used:   0.0 secs
Memory used: 3.6 Mb (3804656 bytes)
Writing basic solution to 'C:\Users\gonzalo\AppData\Local\Temp\tmpz21x0ld7.glpk.raw'...
8243 lines were written
```

Fig. 11. PYOMO software with ADAM solver processing.

Fig. 12 shows the generation profile of the system. This graph has been arranged with the base units at the bottom. The first is hydro generation, which produces at a rate of 9600 MWh per period, giving an output of 230,400 MWh at the end of the planning horizon, followed by nuclear generation with an hourly output of 1755 MWh, for a total of 42,120 MWh. This is followed by the thermal units produced from natural gas, with a variable production that has its minimum in hours 5 to 8 (less than 2,000 MWh in each period), the production starts to increase in hour 15 with 5,774.7 MWh and has its maximum in the last hour with 6345.157 MWh. The total production from this source is 100 291.4 MWh. In **Fig. 13** it can be seen in more detail that the wind generation has a lot of variation, the highest values are registered between hours 1-2, 9-14. The hourly maximum occurs at 11 o'clock with a value of 596.2 MWh and the total generation from this source is 4,481.1 MWh. Finally, solar energy starts producing electricity at 8 o'clock, generates a maximum between 12 and 16 o'clock with an hourly average of 191 MWh, and stops producing at 20 o'clock. The total production of this source is 1,707.5 MWh. The other sources that do not appear in this production profile are those that have not produced any electricity.

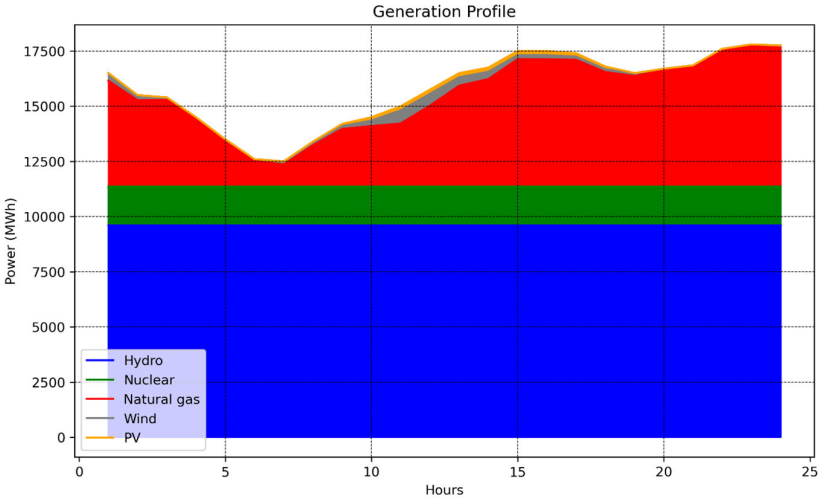

Fig. 12. Generation profile for the whole programming horizon.

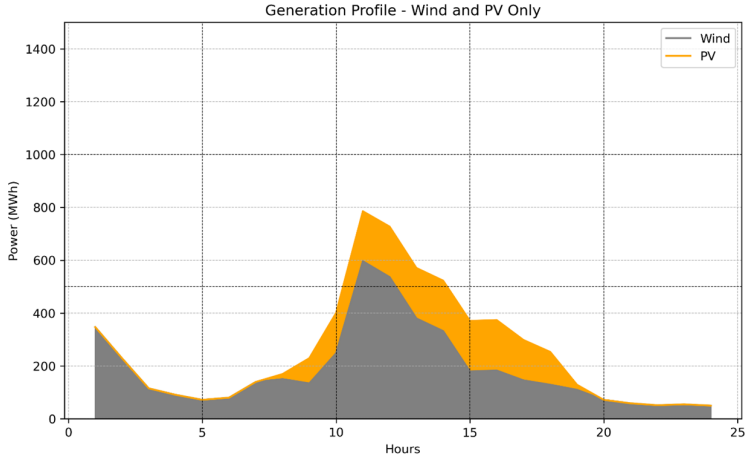

Fig 13. Generation profile for PV and wind sources.

To get a better idea of the importance of each region, it is important to look at the importance per bus for each type of generation. **Fig. 14** shows the generation per bus for each type of source. Bus E1 (Northwest Argentina region) has a total generation of 1294 MWh, with a predominance of hydro (969 MWh). For bus E2 (Argentine Northeast region) there is only hydro generation with a total of 19764 MWh. Bus E3 (Northwest Argentina region) also has only hydro generation with a total of 46116 MWh. Bus E4 (Northeastern Argentina) has a greater diversity of sources, with hydroelectricity producing 1454 MWh, wind 207.9 MWh, and solar 278.9 MWh, but this bus belongs to a region with high wind speeds and a high availability of clear days (La Rioja province). Bus E5 (central region) has a total production of 11662 MWh, with significant production of the natural gas thermal source of 11380 MWh and wind power of 114 MWh together with the other renewable, (PV), of 168 MWh. The E6 bus (central region) has a total production of 20008 MWh, with hydro at 4032 MWh, nuclear at 15552 MWh, wind at 172 MWh, and PV at 252 MWh. For the E7 bus (Litoral region), there is only hydro production of 13608 MWh. Finally, for this figure, in bus E8 (Litoral region), there is also hydro production with a total of 9072 MWh.

Fig. 15 shows the production of buses 9 to 15. For the first bus (E9, Cuyo region) there is a total generation of 25220 MWh, where there are thermal sources with 14797 MWh, hydro with 9600 MWh, and PV with 822 MWh. For bus E10 (Buenos Aires region) there is a total of 102193 MWh, with 74113 MWh from thermal, 26568 MWh from nuclear, and 1511 MWh from wind. Bus E11 (Comahue region) has a total production of 34020 MWh, where only hydro sources are registered, for Bus E12 of the same region there are 79380 MWh from the same source. Bus E13 has a hydro production of 7430 MWh and a wind production of 1401 MWh. Bus E14 has a hydro production of 3715.2 MWh and a wind production of 700 MWh, while bus E15 has a hydro production of 1238.4 MWh and a wind production of 233 MWh. The last 3 buses belong to the Patagonia region and are characterized by the presence of important winds. **Fig. 16** shows the details of generation by bus from E1 to E9, but only for renewable sources. **Fig. 17** does the same for buses E9 to E15.

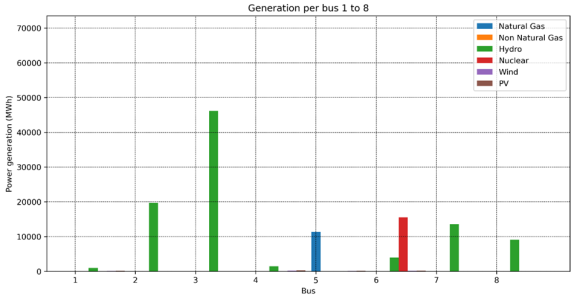

Fig. 14. Generation per bus 1-8 for all sources.

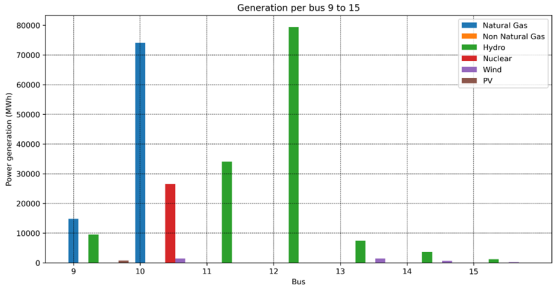

Fig. 15. Generation per bus 9-15 for all sources.

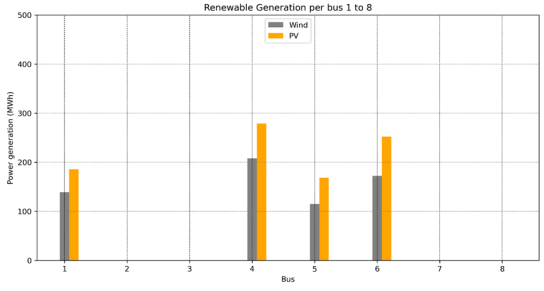

Fig. 16. Generation per bus 1-8 for renewable sources.

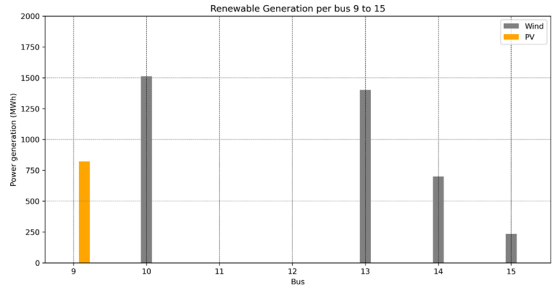

Fig. 17. Generation per bus 9-15 for renewable sources.

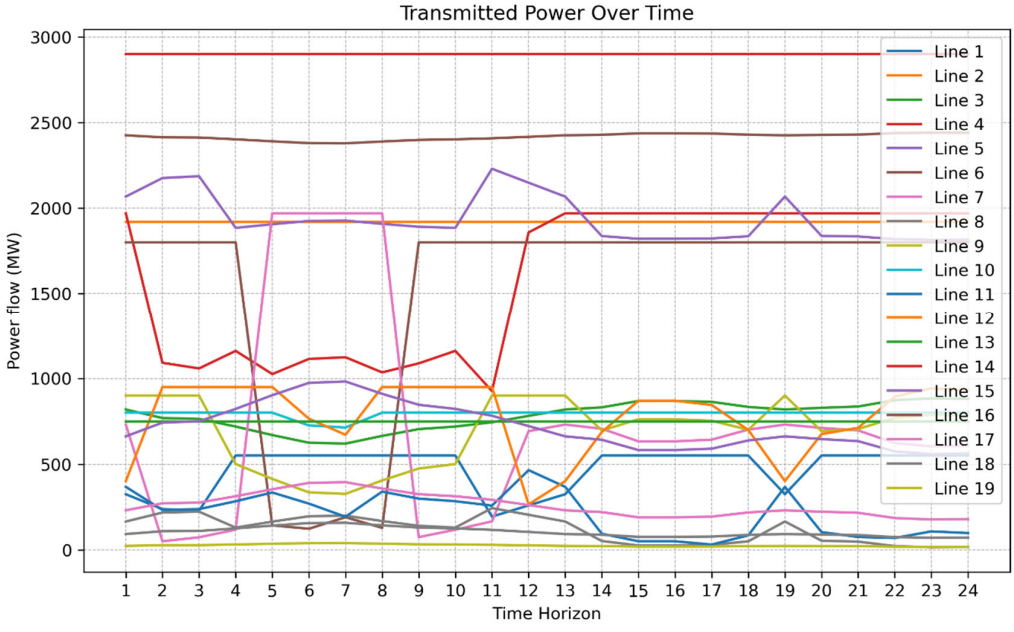

Fig 18. Transmitted power for the whole system.

Fig. 18 shows the power transmitted by each of the lines. The line with the highest flow is line 16 with a total of 58014 MW, followed by line 5 with 46528 MW, then line 2 with 46080 MW, line 15 with a total of 38248 MW, line 14 with 36584 MW and line 13 with 19039 MW. The remaining lines have lower flows, the lowest being line 18 with 2491 MW and line 19 with 622 MW. The location of the lines about the scheme and the buses E1-E15 are described in Table A4 in (G. Alvarez, 2020a).

6. Conclusions

This paper presents a comprehensive approach to the problem of integrating renewable energy sources into very large-scale electrical systems. The goal of the research is to lessen the impact of intermittent power sources, including solar and wind, on the stability and dependability of systems. An innovative mathematical model is put forth that combines conventional and renewable energy sources, allowing for comprehensive power generation control. The new model, which forecasts generation from renewable sources, combines neural network modeling, classical optimization, and moder method to attend large scale systems, as the block modeling methodology. The novel approach makes it easier to adjust the amount of power produced while considering realistic considerations such transmission variances, system demand, and reserves.

The viability and efficacy of the proposal are proved by applying it to the Argentine Power System, with over 45 million habitants. Analysis of the generation and transmission dynamics in various regions yields important insights into how energy resources are allocated and used within the system. The comprehension and implementation of renewable energy integration techniques are greatly influenced by the findings of this study. In their pursuit of a more resilient and sustainable energy framework, it offers direction to engineers, energy planners, decision-makers in the power industry, and other relevant parties.

References

Abdou, I., & Tkiouat, M. (2018). Unit Commitment Problem in Electrical Power System: A Literature Review. *International Journal of Electrical and Computer Engineering (IJECE)*, *8*(3), 1357. https://doi.org/10.11591/ijece.v8i3.pp1357-1372

Ahmad, T., Zhang, H., & Yan, B. (2020). A review on renewable energy and electricity requirement forecasting models for smart grid and buildings. *Sustainable Cities and Society*, *55*, 102052. https://doi.org/10.1016/j.scs.2020.102052

Ahmed, S. D., Al-Ismail, F. S. M., Shafiullah, M., Al-Sulaiman, F. A., & El-Amin, I. M. (2020). Grid Integration Challenges of Wind Energy: A Review. *IEEE Access*, *8*, 10857–10878. https://doi.org/10.1109/ACCESS.2020.2964896

Akella, A. K., Saini, R. P., & Sharma, M. P. (2009). Social, economical and environmental impacts of renewable energy systems. *Renewable Energy*, *34*(2), 390–396. https://doi.org/10.1016/j.renene.2008.05.002

Alguacil, N., Membel, S., Conejo, a J., & Membel, S. (2000). Multiperiod Optimal Power Flow Using Benders Decomposition. *Power Systems, IEEE Transactions On*, *15*(1), 196–201. https://doi.org/10.1109/59.852121

Alvarez, G. (2020a). Integrated scheduling from a diversity of sources applied to the Argentine electric power and natural gas systems. *Computers & Chemical Engineering*, *134*, 106691. https://doi.org/10.1016/j.compchemeng.2019.106691

Alvarez, G. (2020b). Operation of pumped storage hydropower plants through optimization for power systems. *Energy*, *202*, 117797. https://doi.org/10.1016/j.energy.2020.117797

Alvarez, G. (2020c). Optimization analysis for hydro pumped storage and natural gas accumulation technologies in the Argentine Energy System. *Journal of Energy Storage*, *31*(June), 101646. https://doi.org/10.1016/j.est.2020.101646

Alvarez, G. (2022a). Integrated modeling of the peer-to-peer markets in the energy industry. *International Journal of Industrial Engineering Computations*, *13*(1), 101–118. https://doi.org/10.5267/j.ijiec.2021.7.002

Alvarez, G. (2022b). Stochastic optimization considering the uncertainties in the electricity demand, natural gas infrastructures, photovoltaic units, and wind generation. *Computers & Chemical Engineering*, *160*, 107712. https://doi.org/10.1016/j.compchemeng.2022.107712

Alvarez, G., & Blas, M. J. (2021). Optimization of electric power systems considering the environmental impact and uncertainties. *2021 Third International Sustainability and Resilience Conference: Climate Change*, 416–423. https://doi.org/10.1109/IEEECONF53624.2021.9667979

Alvarez, G. E. (2021). A multi-objective formulation of improving flexibility in the operation of electric power systems: Application to mitigation measures during the coronavirus pandemic. *Energy*, *227*, 120471. https://doi.org/10.1016/j.energy.2021.120471

Argentine Atomic Energy Commission (CNEA). (2016). *Synthesis of the Wholesale Electricity Market of the Republic of Argentina. January*.

Arias, A., Sanchez, J. D., & Granada, M. (2018). Integrated planning of electric vehicles routing and charging stations location considering transportation networks and power distribution systems. *International Journal of Industrial Engineering Computations*, 535–550. https://doi.org/10.5267/j.ijiec.2017.10.002

Bachy, B., & Franke, J. (2015). Modeling and optimization of laser direct structuring process using artificial neural network and response surface methodology. *International Journal of Industrial Engineering Computations*, *6*(4), 553–564. https://doi.org/10.5267/j.ijiec.2015.4.003

Bagherian, M. A., & Mehranzamir, K. (2020). A comprehensive review on renewable energy integration for combined heat and power production. *Energy Conversion and Management*, *224*, 113454. https://doi.org/10.1016/j.enconman.2020.113454

BBC. (2021). Climate change: UN to reveal landmark IPCC report findings. *Science-Environment*, 1.

Bharadwa, A. (2020). *Wind Turbine Power Output Forecast*.

Branco, P., Gonçalves, F., & Costa, A. C. (2020). Tailored Algorithms for Anomaly Detection in Photovoltaic Systems. *Energies*, *13*(1), 225. https://doi.org/10.3390/en13010225

Breeze, P. (2014). *Power Generation Technologies* (2nd editio). Elsevier. https://doi.org/10.1016/C2012-0-00136-6

Brownlee, J. (2017). *How to use timesteps in LSTM networks for time series forecasting*. Machine Learning Mastery.

Burton, T., Jenkins, N., Sharpe, D., & Bossanyi, E. (2011). Wind Energy Handbook, Second Edition. In *Wind Energy Handbook, Second Edition*. John Wiley & Sons, Ltd. https://doi.org/10.1002/9781119992714

CAMMESA. (2019). Report February 2019. In *Monthly report - Main variables of the month*. https://doi.org/10.18356/fc4b62a8-es

CAMMESA. (2023). *Generación de Renovables*. Generación Por Tecnología. https://cammesaweb.cammesa.com/generacion-real/

Carrion-i-Silvestre, J. L., & Kim, D. (2019). Quasi-likelihood ratio tests for cointegration, cobreaking, and cotrending. *Econometric Reviews*, *38*(8), 881–898. https://doi.org/10.1080/07474938.2018.1528416

Chen, C. H., Chen, N., & Luh, P. B. (2017). Head Dependence of Pump-Storage-Unit Model Applied to Generation Scheduling. *IEEE Transactions on Power Systems*, *32*(4), 2869–2877. https://doi.org/10.1109/TPWRS.2016.2629093

Chen, P.-Y., Chen, S.-T., Hsu, C.-S., & Chen, C.-C. (2016). Modeling the global relationships among economic growth, energy consumption and CO2 emissions. *Renewable and Sustainable Energy Reviews*, *65*, 420–431. https://doi.org/10.1016/j.rser.2016.06.074

Erisen, B. (2018). *Wind Turbine Scada Dataset*. Scada Data of a Wind Turbine in Turkey. https://www.kaggle.com/datasets/berkerisen/wind-turbine-scada-dataset

Farrokhtala, A., Chen, Y., & Hu, T. (2019). The Time Element of Temporal Networks. *2019 IEEE Global Communications Conference (GLOBECOM)*, 1–6. https://doi.org/10.1109/GLOBECOM38437.2019.9013412

Foley, A. M., Leahy, P. G., Marvuglia, A., & McKeogh, E. J. (2012). Current methods and advances in forecasting of wind power generation. *Renewable Energy*, *37*(1), 1–8. https://doi.org/10.1016/j.renene.2011.05.033

Hart, W. E., Watson, J.-P., & Woodruff, D. L. (2011). Pyomo: modeling and solving mathematical programs in Python. *Mathematical Programming Computation*, *3*(3), 219–260. https://doi.org/10.1007/s12532-011-0026-8

Homan, S., Mac Dowell, N., & Brown, S. (2021). Grid frequency volatility in future low inertia scenarios: Challenges and mitigation options. *Applied Energy*, *290*, 116723. https://doi.org/10.1016/j.apenergy.2021.116723

Horváth, L., Kokoszka, P., & Rice, G. (2014). Testing stationarity of functional time series. *Journal of Econometrics*, *179*(1), 66–82. https://doi.org/10.1016/j.jeconom.2013.11.002

IPCC - Contribution of Working Group I to the Sixth Assessment Report of the Intergovernmental Panel on Climate Change. (2021). *Summary for Policymakers. In: Climate Change 2021: The Physical Science Basis.*

Jangir, P., Manoharan, P., Pandya, S., & Sowmya, R. (2023). MaOTLBO: Many-objective teaching-learning-based optimizer for control and monitoring the optimal power flow of modern power systems. *International Journal of Industrial Engineering Computations*, *14*(2), 293–308. https://doi.org/10.5267/j.ijiec.2023.1.003

Kagemoto, H. (2020). Forecasting a water-surface wave train with artificial intelligence- A case study. *Ocean Engineering*, *207*, 107380. https://doi.org/10.1016/j.oceaneng.2020.107380

Kim, B., & Kim, J. (2020). Adjusting Decision Boundary for Class Imbalanced Learning. *IEEE Access*, *8*, 81674–81685. https://doi.org/10.1109/ACCESS.2020.2991231

Kumar, M. (2020). Social, Economic, and Environmental Impacts of Renewable Energy Resources. In *Wind Solar Hybrid Renewable Energy System* (Vol. 151, pp. 1298–1306). IntechOpen. https://doi.org/10.5772/intechopen.89494

Kumar, R., Sharma, A. Kr., & Tewari, P. C. (2012). Markov approach to evaluate the availability simulation model for power generation system in a thermal power plant. *International Journal of Industrial Engineering Computations*, *3*(5), 743–750. https://doi.org/10.5267/j.ijiec.2012.08.003

Li, X., Li, T., Wei, J., Wang, G., & Yeh, W. W. G. (2014). Hydro unit commitment via mixed integer linear programming: A case study of the three gorges project, China. *IEEE Transactions on Power Systems*, *29*(3), 1232–1241. https://doi.org/10.1109/TPWRS.2013.2288933

Livieris, I. E., Stavroyiannis, S., Pintelas, E., & Pintelas, P. (2020). A novel validation framework to enhance deep learning models in time-series forecasting. *Neural Computing and Applications*, *32*(23), 17149–17167. https://doi.org/10.1007/s00521-020-05169-y

Neshat, M., Nezhad, M. M., Abbasnejad, E., Mirjalili, S., Tjernberg, L. B., Astiaso Garcia, D., Alexander, B., & Wagner, M. (2021). A deep learning-based evolutionary model for short-term wind speed forecasting: A case study of the Lillgrund offshore wind farm. *Energy Conversion and Management*, *236*, 114002. https://doi.org/10.1016/j.enconman.2021.114002

Nuclear Energy Agency. (2011). *Technical and Economic Aspects of Load Following with Nuclear Power Plants*.

Orlov, A., Sillmann, J., & Vigo, I. (2020). Better seasonal forecasts for the renewable energy industry. *Nature Energy*, *5*(2), 108–110. https://doi.org/10.1038/s41560-020-0561-5

Overbye, T. J., Cheng, X., & Sun, Y. (2004). A comparison of the AC and DC power flow models for LMP calculations. *Proceedings of the 37th Annual Hawaii International Conference on System Sciences*, 9. https://doi.org/10.1109/HICSS.2004.1265164

Panos, E., & Lehtilä, A. (2016). *Dispatching and unit commitment features in TIMES*.

Phillips, P. C. B., & Ouliaris, S. (1990). Asymptotic Properties of Residual Based Tests for Cointegration. *Econometrica*, *58*(1), 165. https://doi.org/10.2307/2938339

Poorvaezi Roukerd, S., Abdollahi, A., & Rashidinejad, M. (2020). Uncertainty-based unit commitment and construction in the presence of fast ramp units and energy storages as flexible resources considering enigmatic demand elasticity. *Journal of Energy Storage*, *29*, 101290. https://doi.org/10.1016/j.est.2020.101290

Rakhmonov, I. U., & Reymov, K. M. (2020). Statistical models of renewable energy intermittency. *E3S Web of Conferences*, *216*, 01167. https://doi.org/10.1051/e3sconf/202021601167

Raybaut, P. (2009). *Spyder-documentation*.

Sahoo, A. K., Rout, A. K., & Das, D. K. (2015). Response surface and artificial neural network prediction model and optimization for surface roughness in machining. *International Journal of Industrial Engineering Computations*, *6*(2), 229–240. https://doi.org/10.5267/j.ijiec.2014.11.001

Shahidehpour, M., Yamin, Hatim., & Li, Zuyi. (2003). Market Operations in Electric Power Systems. In *Market Operations in Electric Power Systems*. Institute of Electrical and Electronics Engineers, Wiley-Interscience. https://doi.org/10.1002/047122412x

Silva, R. P., Zarpelão, B. B., Cano, A., & Junior, S. B. (2021). Time Series Segmentation Based on Stationarity Analysis to Improve New Samples Prediction. *Sensors*, *21*(21), 7333. https://doi.org/10.3390/s21217333

Sinsel, S. R., Riemke, R. L., & Hoffmann, V. H. (2020). Challenges and solution technologies for the integration of variable renewable energy sources—a review. *Renewable Energy*, *145*, 2271–2285. https://doi.org/10.1016/j.renene.2019.06.147

Stott, B., Jardim, J., & Alsac, O. (2009). DC Power Flow Revisited. *IEEE Transactions on Power Systems*, *24*(3), 1290–1300. https://doi.org/10.1109/TPWRS.2009.2021235

Sun, L., Du, J., Gao, T., Lu, Y.-D., Tsao, Y., Lee, C.-H., & Ryant, N. (2018). A Novel LSTM-Based Speech Preprocessor for Speaker Diarization in Realistic Mismatch Conditions. *2018 IEEE International Conference on Acoustics, Speech and Signal Processing (ICASSP)*, 5234–5238. https://doi.org/10.1109/ICASSP.2018.8462311

U.S. Energy Information Administration. (2017). Average Power Plant Operating Expenses for Major U.S. Investor-Owned Electric Utilities, 2007 through 2017. In *Electric Power Annual* (p. 239). U.S. Department of Energy.

Van Den Bergh, K., Delarue, E., & D'haeseleer, W. (2014). DC power flow in unit commitment models. *TME Working Paper-Energy and Environment, Tech. Rep*.

Wang, H., Liu, Y., Zhou, B., Li, C., Cao, G., Voropai, N., & Barakhtenko, E. (2020). Taxonomy research of artificial intelligence for deterministic solar power forecasting. *Energy Conversion and Management*, *214*, 112909. https://doi.org/10.1016/j.enconman.2020.112909

Weyn, J. A., Durran, D. R., & Caruana, R. (2020). Improving Data-Driven Global Weather Prediction Using Deep Convolutional Neural Networks on a Cubed Sphere. *Journal of Advances in Modeling Earth Systems*, *12*(9). https://doi.org/10.1029/2020MS002109

Yan, H., & Ouyang, H. (2018). Financial Time Series Prediction Based on Deep Learning. *Wireless Personal Communications*, *102*(2), 683–700. https://doi.org/10.1007/s11277-017-5086-2

Yeh, C.-K., Rice, G., & Dubin, J. A. (2023). Functional spherical autocorrelation: A robust estimate of the autocorrelation of a functional time series. *Electronic Journal of Statistics*, *17*(1). https://doi.org/10.1214/23-EJS2112

Zhang, J., Yan, J., Infield, D., Liu, Y., & Lien, F. (2019). Short-term forecasting and uncertainty analysis of wind turbine power based on long short-term memory network and Gaussian mixture model. *Applied Energy*, *241*, 229–244. https://doi.org/10.1016/j.apenergy.2019.03.044

Zhang, M., Zhang, X., Guo, S., Xu, X., Chen, J., & Wang, W. (2021). Urban micro-climate prediction through long short-term memory network with long-term monitoring for on-site building energy estimation. *Sustainable Cities and Society*, *74*, 103227. https://doi.org/10.1016/j.scs.2021.103227

Zhao, J., Tang, Y. H., Wang, L., & Liu, D. C. (2014). The Balance of Power System Peak Load Regulation Considering the Participation of Nuclear Power Plant. *Applied Mechanics and Materials*, *672–674*, 477–481. https://doi.org/10.4028/www.scientific.net/amm.672-674.477